GRC Transactions, Vol. 41, 2017

SAND2017-5777C

Advanced Percussive Drilling Technology for Geothermal Exploration and Development

DE-FOA-EE0005502

Jiann Su, David W. Raymond and Somuri Prasad

Sandia National Labs <Author Style>

Dale Wolfer

Atlas Copco Secoroc <Author Style>

Keywords

Advanced drilling technology, high-temperature drilling

ABSTRACT

Percussive hammers are a promising advance in drilling technology for geothermal since they rely upon rock reduction mechanisms that are well-suited for use in the hard, brittle rock characteristic of geothermal formations. Also known as down-the-hole (DTH) hammers, they are also compatible with low-density fluids that are often used for geothermal drilling. Experience in mining and oil and gas drilling has demonstrated their utility for penetrating hard rock. One limitation to more wide-scale deployment is the ability of the tools to operate at high temperatures (~300°C) due to elastomers used in the construction and the lubrication required for operation. As part of a United States Department of Energy Funding Opportunity Announcement award, Atlas Copco was tasked with developing a high-temperature DTH capable of being used in geothermal environments. A full-scale development effort including design, build, and testing was pursued for the project. This report summarizes the results of the percussive hammer development efforts between Atlas-Copco Secoroc and Sandia National Labs as part of DE-FOA-EE0005502. Certain design details have been omitted due to the proprietary nature of the information.

1. Introduction

Drilling costs contribute substantially to geothermal electricity production costs. A geothermal well construction technology evaluation study sponsored by the Department of Energy Office of Geothermal Technologies has shown that drilling services and consumables can exceed 50% of total construction costs for deep geothermal wells (Polsky). Since drill rig time dominates well drilling costs, technology is needed that improves rate of penetration (ROP) and is capable of drilling exploration and production wells to depth.

Geothermal drilling is notable for the combination of hard/abrasive fractured rock formations, high temperatures, and the frequent loss of circulated drilling fluids to the formation. Presently, rock reduction methods used in geothermal drilling include using tungsten-carbide-insert roller cone bits, polycrystalline diamond compact (PDC) bits, and diamond impregnated drag bits. Although PDC bits account for 65-70% of all footage drilled today in the oil and gas industry, advances in PDC bit technology indicate a substantive future role of the bits in geothermal applications, presently their use is very limited (Polsky).

Rock reduction in conventional geothermal well construction is dominated by roller cone bits. While this technology has served the industry well with capability of drilling the varied rock types found in geothermal formations, roller cones are subject to slow penetration rates (10-20 ft/hr) and limited bit life (< 40 hours) under the rigors of hard-rock, high-temperature, abrasive rock drilling. Lubricated bearings and accompanying seals support the roller cones. Since cone rotation is required for rock crushing, cone seizure will render the entire bit inoperative. Seal failure usually leads to bearing failure as the seals protect bearings that can fail when exposed to the abrasive cuttings in geothermal formations.

As geothermal drilling continues into deeper and hotter formations for development of both conventional and enhanced geothermal systems, advanced penetration rate drilling technologies must be realized to keep well construction costs manageable.

Percussive drilling is a widely accepted robust technique for penetrating hard rock. Established research has shown that percussive devices have among the lowest mechanical specific energies (energy required to remove a given volume of rock) of drilling methods and an industry reputation for reliably drilling hard rock (Thuro 1996, Kahraman, Bilgin et al. 2003). Pneumatic drilling is particularly advantageous in highly fractured and cavernous rocks where lost circulation is a concern. It is also well suited to hard, dry formations with relatively small amounts of formation liquids.

Pneumatic hammers potentially offer significant cost savings to geothermal well drilling expenditures as they offer remarkable (2x - 10x) rate of penetration performance enhancements over conventional geothermal well drilling solutions. Significant cost savings may be realized as commercially-available down the hole hammer (DTHH) drills are capable of achieving penetration rates of 100 ft/hr in granite – a typical geothermal rock type.

The components of a percussive hammer are relatively simple and reliable in commercial practice. The current state of the technology is seen in the exploded view of an Atlas Copco (AC) hammer shown in Figure 1. Alloy steels are used in the bit body/shank, the piston, and the overall case. Polymers are used for the manufacturer of some components in conventional hammers to mitigate the effects of high impact and to effectively port the compressed gas throughout the hammer for improved power delivery. Elastomers are used throughout the hammer to seal the assembly. The bits are fitted with tungsten carbide inserts that accommodate the abrasive interaction of the percussive hammer with the rock formations at the interface of the hammer with the formation facilitating the rock reduction process. Compressed air accelerates the piston into the bit which in turn strikes the rock to generate cuttings.

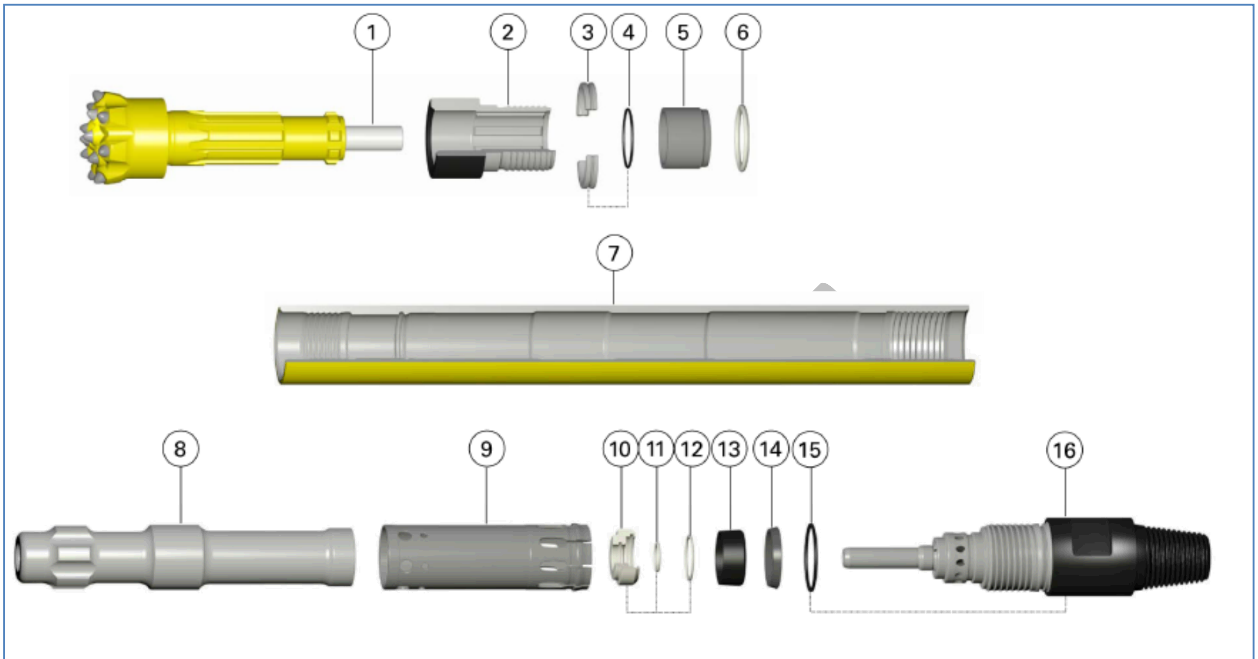

Figure 1. Exploded view of Atlas Copco hammer identifying primary hammer components including the bit assembly (top), hammer case (middle) and piston/feed tube assembly (bottom).

Although existing pneumatic hammer product lines may be able to penetrate typical geothermal formations, the down hole temperatures of geothermal wells (100 – 300°C) can challenge the elastomeric and polymer-based components that are used in the tools. Hence, they are unable to survive the "soak temperatures" encountered in a geothermal well. Additionally, the metal alloy components comprising a percussive hammer may potentially be compromised with reduced strength and fatigue life at elevated temperatures

The proposed advancements to develop a high temperature compatible hammer will address the existing operational limitations of the percussive hammer. The primary intent is to develop an elastomer-less/polymer-less hammer design that maintains the fundamental characteristics of the hammer with effective power delivery necessary to penetrate typical geothermal formations. The performance goals for the tool are target operating temperature up to 300°C with a target rate of penetration (ROP) of 100 ft/hr.

2. Tool Design and Development

2.1 Proof of Concept Bit Development

A hammer assembly consists of two primary components: the hammer itself and the bit. A typical hammer bit is shown in Figure 2. The cutting surface is composed of buttons that are inserted into the bit body which is typically an alloy steel selected for high toughness and hardness. Tungsten carbide is commonly used for the inserts. The body and the inserts are assembled by shrink-fitting or brazing the inserts into openings cut out of the body.

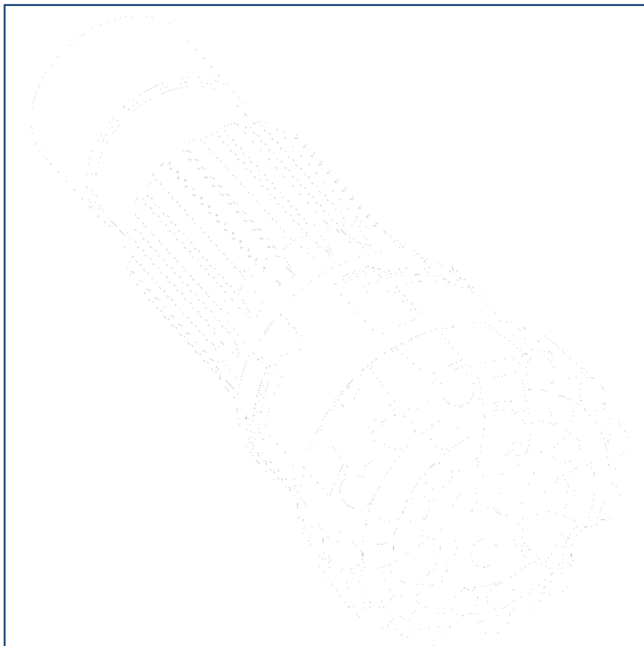

Figure 2. Hammer bit illustration

Early in the development phase, one of the primary concerns was the reliability of the bit operating at high temperature. Under conventional operating temperatures and conditions, the interference fit works well for retaining the buttons. However, temperatures expected in the geothermal wells under consideration are sufficient to cast doubt on the reliability of interference-fit percussive drill bit inserts.

Initial shrink-fit analysis indicated that positive contact pressure would be maintained throughout the expected temperature range. Hoowever there is uncertainty about whether that pressure is adequate to secure the buttons when operating at temperature. The forces produced by shock loading caused by the piston striking the bit create a challenging simulation environment.

The shock forces between the piston and the bit are dependent on the contact time and other factors. Utilizing shock and vibration testing capabilities at Sandia, a test was devised to determine whether the interference fits would be sufficient for retaining the inserts when operating at temperature.

A test fixture was designed to simulate the variable contact stresses between the body and the inserts (Figure 3.) The size of the body was selected to replicate the mass of a bit. Nine ∅0.875” holes, 1.5” apart on a 3x3 pattern were drilled on one face of the body. The inserts are nominally 0.875” tungsten carbide inserts. Each insert was tailored to a specific hole in the body. The hole diameters were individually measured after the initial machining process. The inserts were then ground to give the desired fits. The test fixture as-built is shown in Figure 3.

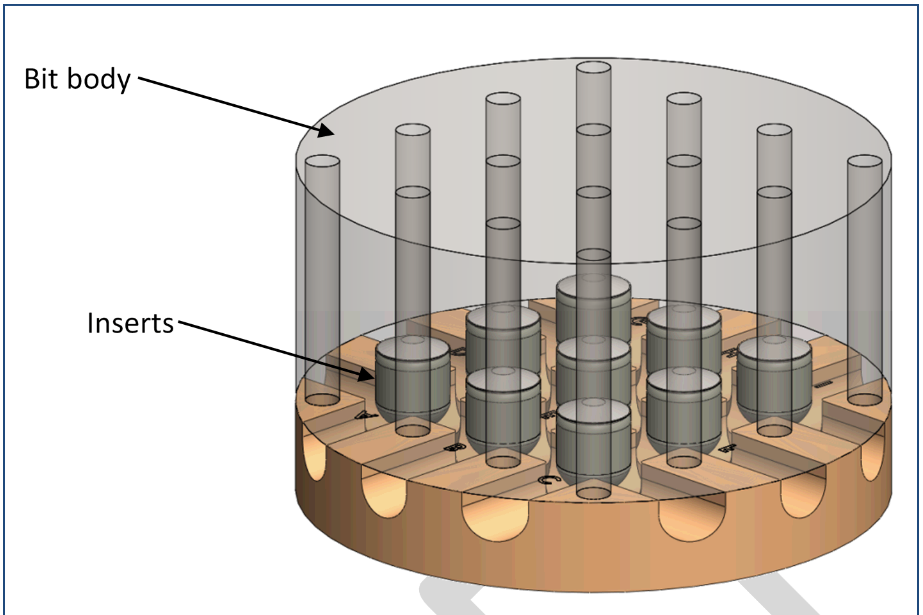

Figure 3. Button test fixture illustration

Before the shock testing began, a baseline measurement of the test fixture and the button locations was made using a coordinate measurement machine (CMM). The CMM gives geometric information about each of the measured features including position in 3-D space. This information is used to determine whether the inserts have moved from their initial positions.

The shock loading test plan is shown in Table 1. The maximum shock level of 12,000 g was chosen based on the equipment capabilities and loading estimates. Since there was some uncertainty as to what would happen, 5 repetitions were chosen for that test. Subsequently, for tests 2-5, 10 repetitions of each level were executed. A visual inspection of the fixture was made between each repetition.

Table 1. Button shock loading test plan

Test #	Shock Amplitude	Shock Duration	Repetitions
1	2500 g (+/- 15%)	0.3ms (+/- 50%)	5
2	5000 g (+/- 15%)	0.3ms (+/-50%)	10
3	7500 g (+/- 15%)	0.3ms (+/-50%)	10
4	10000 g (+/- 15%)	0.3ms (+/-50%)	10
5	12000 g (+/- 15%)	0.3ms (+/-50%)	10

None of the inserts showed measurable movement up to the 7500 g shock load. After Test 4, (10,000 g) inserts H and I began to extract from the hole. Visual inspection after the tests suggested the inserts were moving. The CMM measurement confirmed what was suspected through visual inspection. Results from the testing indicated that button retention

At 12,000 g, additional extraction was seen in I with additional movement seen in H (Figure 4.) Both of these inserts would have been categorized as failing.

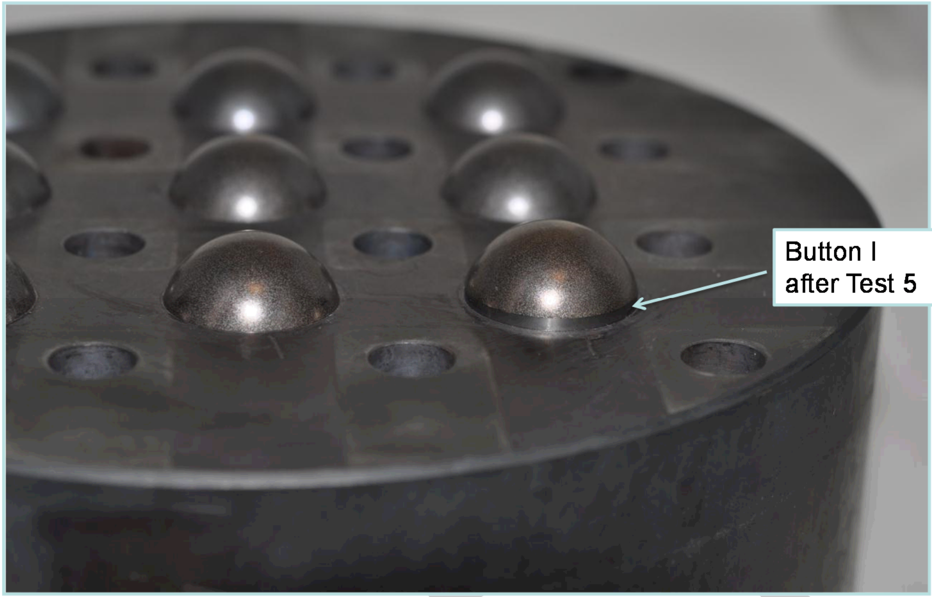

Figure 4. Button extraction after maximum shock loading

These results indicate that for shock loading up to 12,000 g's, the inserts will remain in place even at temperature increases up to 600°F. The interference fit used in the current installation techniques will be acceptable for bits operating in a geothermal thermal environment.

2.2 Tribological Evaluation

Another key element of the high-temperature DTH development was addressing the lubrication challenges. Conventional hammer operation requires injecting medium weight rock drill oil (ISO 220) during operation. While suitable for room temperature testing, it should be noted that it is not suitable for HT operations since target temperatures will seriously degrade the lubricant and can potentially cause it to flash.

Alternative lubricious coatings suitable for the target operating conditions were evaluated and examined by the Sandia Materials R&D Department. Coupon-level testing of the solid lubricants was performed on metal substrates representing the hammer components. A high temperature tribometer (Figure 5) capable of making friction and wear measurements up to 300°C was designed and fabricated to characterize the lubricious behavior of the coatings. Tests were conducted under atmospheric conditions.

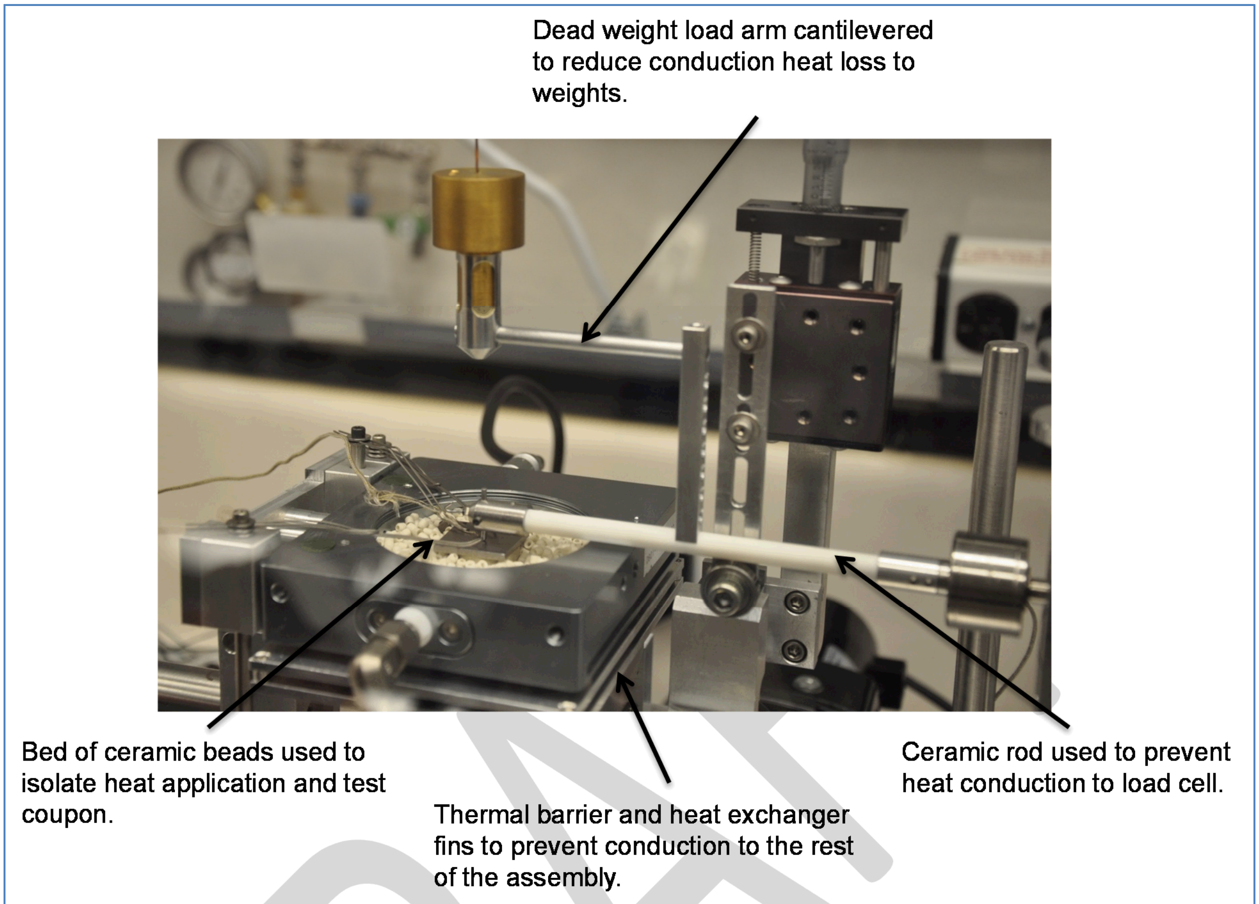

Figure 5. High-temperature tribometer for friction and wear

First, an uncoated hardened tool steel was tested at 300°C. Friction was high with coefficient of friction (CoF) around 0.6. A cross section of the wear scar suitable for transmission electron microscopy (TEM) was prepared by focused ion beam microscopy (FIB). The FIB cut was made in the center of the wear surface along the direction of sliding. Results show that the surface was heavily oxidized. The depth of the oxidized layer can be gaged from the TEM micrograph (Figure 6). The phenomenon is called tribo-oxidation.

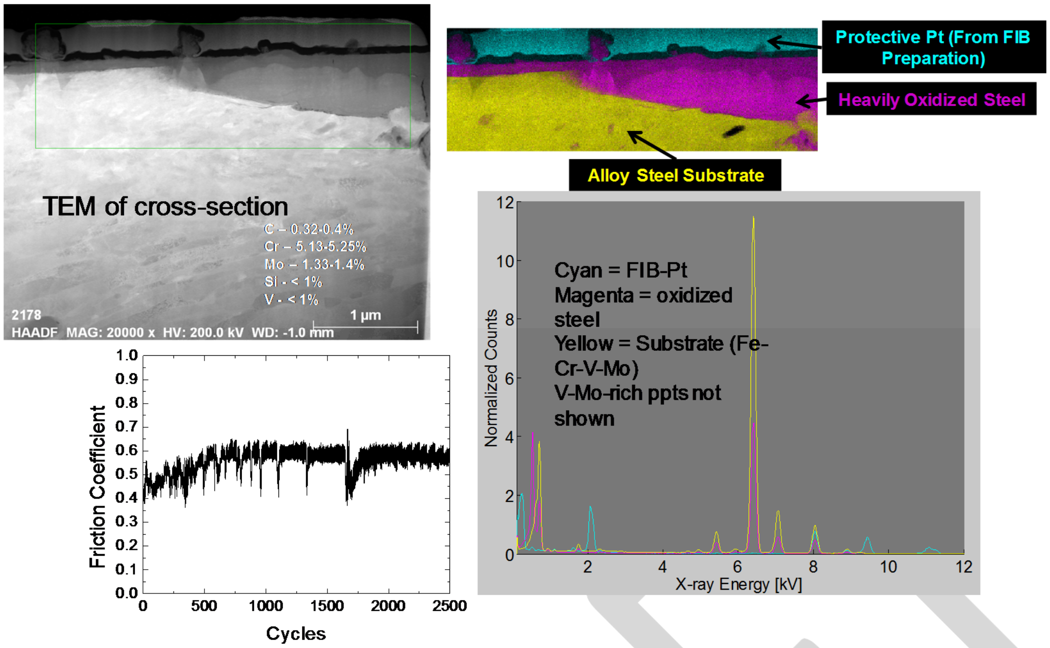

Figure 6. Uncoated tool steel tested at 300°C

Figure 7 shows the friction and cross-sectional TEM data on the same substrate with a diamond-like carbon (DLC) solid lubricant. The DLC is an amorphous mix of diamond-like and quartz like networks, essentially a nanocomposite. A ceramic barrier layer was introduced between the steel substrate and the DLC. Note that the friction reduced progressively with cycles of sliding, reaching very low values of the order of 0.05 to 0.1.

Raman analysis was carried out to confirm whether frictional contact had introduced chemical changes to DLC that were beneficial. The CoF is changing with time, but is decreasing not increasing as one might expect. The top two images of Figure 7 correspond to TEM of a typical cross-section with corresponding spectral image map. Tribo-oxidation was significantly reduced. There was practically no plastic deformation in the steel substrate. There also was no apparent loss (wear) of thickness in DLC.

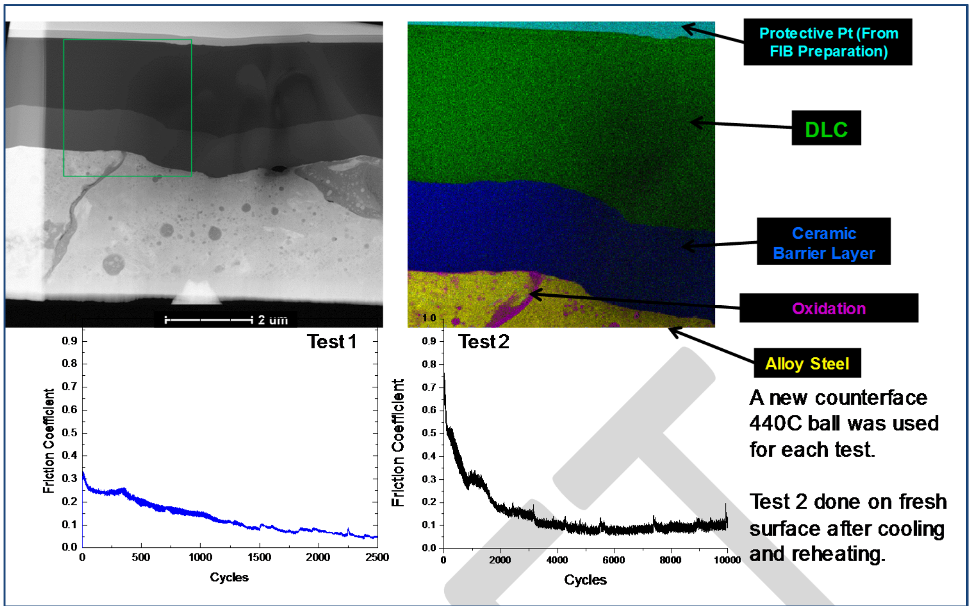

Figure 7. DLC nanocomposite on ceramic layer

Scanning electron microscope (SEM) and spectral images of wear surfaces (left) and transfer films on steel balls (right) are shown in Figure 8. Again, there was no observable loss of material seen on the wear surfaces. It is interesting to note that the wear scars appear smoother than the unworn regions on the coating. Spectral images reveal the enrichment of SiO fragments on the wear surfaces. There is also transfer of DLC material onto the steel counter-face, but no significant damage to the ball.

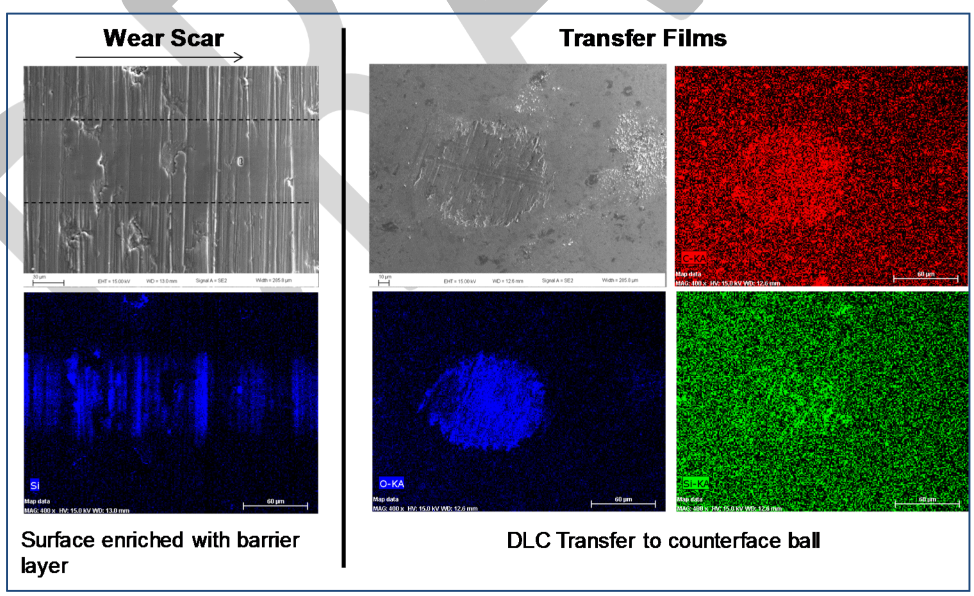

Figure 8. Wear surfaces & transfer films

A typical cross-section of DLC coating with multiple barrier coating (a ceramic layer in blue and nanolamiante in red is shown in Figure 9. Either the residual stresses in the TiCN nanolaminate or friction induced shear stresses begin to induce delamination of the nanolamiante.

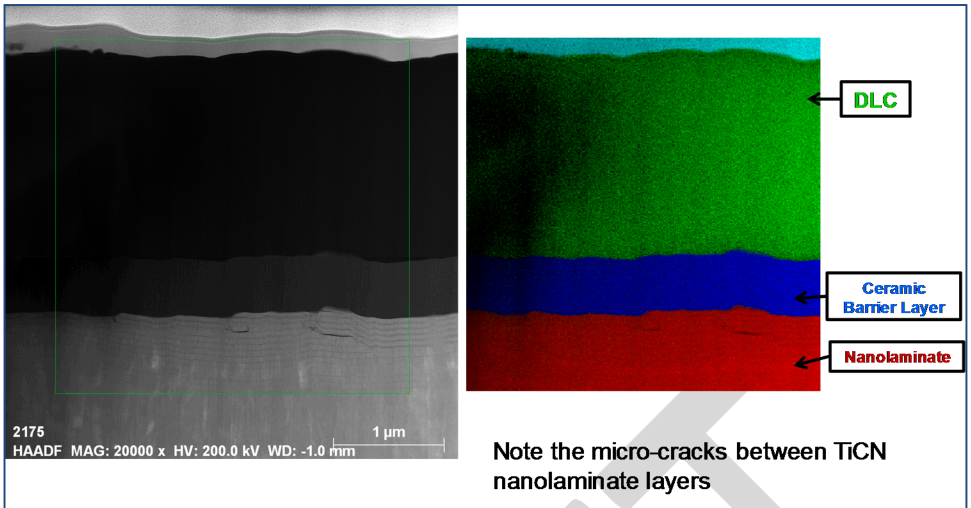

Figure 9. Multilayer Coatings: Load Bearing, Diffusion Barrier / Oxidation Protection

Based on the test coupon-level test results, a nanocomposite DLC with a single ceramic barrier coating was selected as the preferred solid lubricant to mitigate high temperature friction and wear.

2.3 Baseline Design

Atlas Copco Secoroc produced a proof of concept (POC) hammer design having several features aimed at survivability in a high temperature environment and performance against high backpressure as is expected in deep-hole applications. This tool utilizes an operating cycle unlike any used by Secoroc or known competitors, so the performance of the tool must be analyzed and tuned using conventional DTH hammer development methods before placement in high temperature conditions.

In theory, DTH hammers have no limitation in depth or backpressure, so long as inlet pressure in sufficiently high to provide adequate differential pressure across the hammer. In reality, additional volumetric flow, in addition to pressure, is required to maintain an effective rate of advance, since the hammer is exhausting at a higher fluid density that at atmospheric conditions. In practice, conditions of formation fluid influx and other phenomena increase back pressure to the extent that available surface equipment cannot maintain flow and pressure sufficient to maintain effective advance with DTHH. Common practice in oilfield drilling is to switch from DTHH to rotary drilling under such conditions. When the wellbore is drilled past the fluid producing zone, the section is cased and cemented to isolate the undesired fluid producing zone, allowing resumption of drilling with DTHH.

The cycle chosen for the POC hammer is unlike any currently sold by Secoroc, but represents a combination of elements aimed at survivability in high temperatures, efficiency without conventional lubrication, and consistent performance in deep holes without the use of elastomers. These elements include:

- Fixed porting. Flows into and out of chambers is controlled only by piston position. Active valve operation is difficult to achieve without the use of elastomers.

- Constant piloting of the piston in cylinder and bearing. Unlike other piston stem bearing hammer designs, the piston is always supported by two removable internal parts.
- No piston/casing contact. Unlike most hammers, the piston is not piloted inside the casing and in fact never makes contact. This eliminates any need for lubricious treatment of the casing.
- Absence of constant downward piston bias. Most hammer designs feed the return chamber by connecting a portion of the piston area to line pressure. This produces a constant downward force that must be overcome during the return stroke and increases required return area. Absence of this bias allows a smaller return area (and larger/stronger piston stem) to be used.
- Movement of return chamber inlet timing upward to the cylinder, increasing chamber volume; this improves performance against backpressure and increases air consumption.

Initial testing of the low temperature prototype showed a significant drop in ROP against expected values due to internal leakage between the Air Distributor and Cylinder. For low ambient temperature operation, a common, 70 Durometer Buna N o-ring was found to effect a sufficient seal such that hammer performance met target values. Since this solution was not viable for high temperature operation, a suitable sealing method was required. Tests were conducted using high temperature, graphite filled valve packing in lieu of the o-ring. The results are shown graphically below.

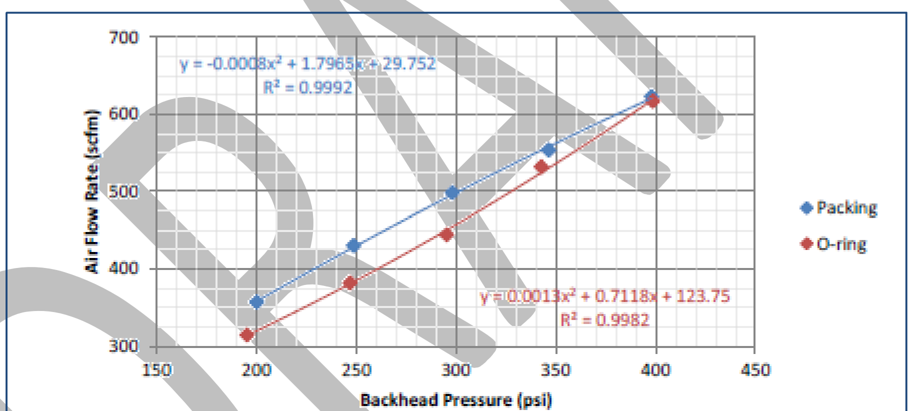

Figure 10. Flow rate vs. backhead pressure

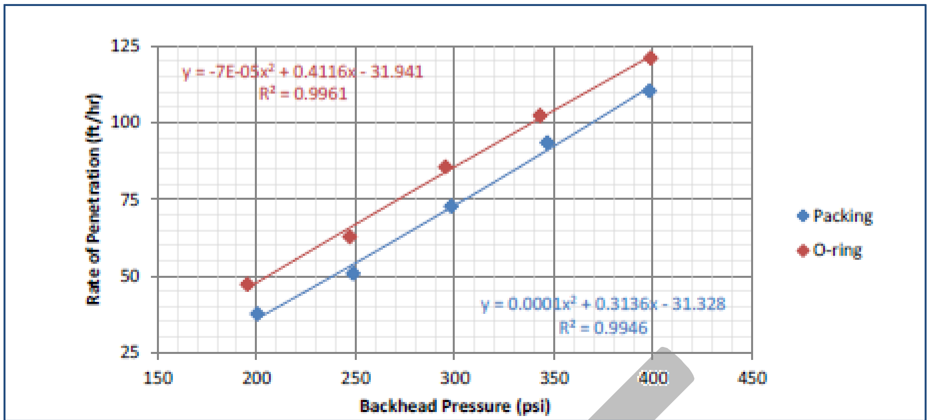

Figure 11. Rate of penetration vs. backhead pressure

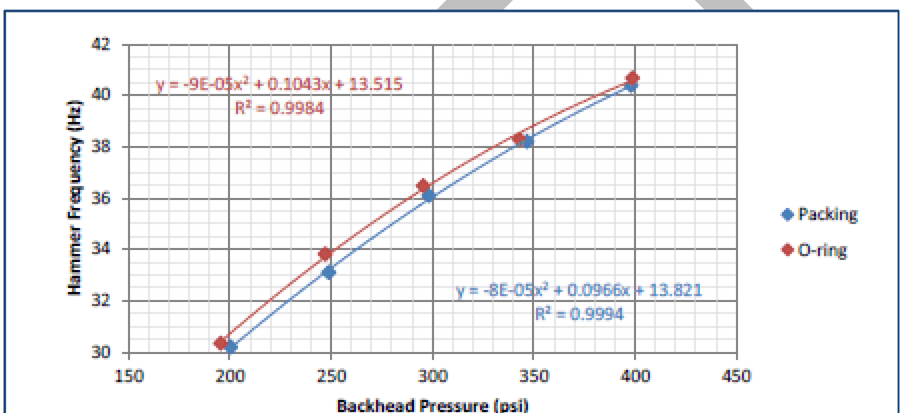

Figure 12. Hammer frequency vs. backhead pressure

These results showed an average increase in air flow of 7.9% and an average decrease in ROP of 39.54% versus a conventional o-ring. About the time these tests were done, a perfluoroelastomer material, Marketed by DuPont as Kalrez® was identified as a good candidate for a sealing element, with a maximum operating temperature of 325 C (617 F). Since this material is a drop-in replacement for the low temperature o-ring, this option was adopted and further work on the valve packing seal was abandoned. It is believed that modifications to the valve packing seal arrangement could achieve better results than observed, but that these results would be unlikely to exhibit any advantageous performance versus the high temperature o-ring.

3. Lab Testing and Results

3.1 Baseline Performance Testing at Atlas Copco Test Cell

Baseline testing of the high temperature prototype was conducted at the test facility at Atlas Copco Secoroc, USA in Roanoke, VA. The test stand is a purpose built, computer controlled drill tower (see Figure 13 and Figure 14). All tests were conducted at ambient temperature. Drilling was conducted in Barre Granite blocks with an unconfined compressive strength of 22ksi (151 MPa). Feed force was maintained constant at 5500 lbf (24.46 kN). Rotation speed was maintained at 40 rpm. A standard, 5.5 inch (140 mm bit fitted with spherical tungsten carbide inserts was used for testing. Testing of the high temperature prototype was conducted using the low temperature prototype as a control.

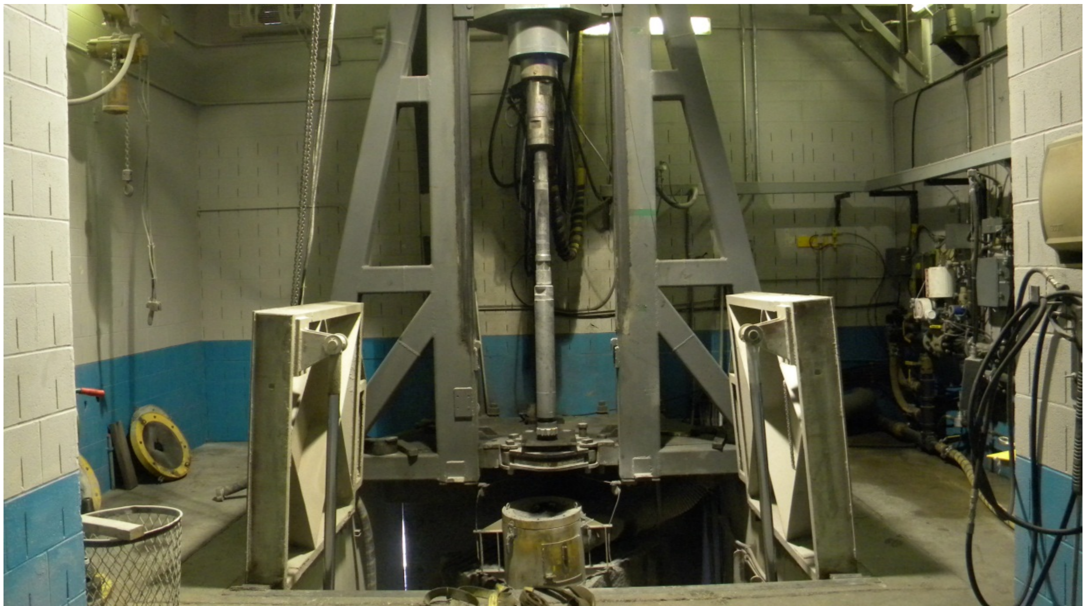

Figure 13. Drill Tower, Showing Basement Access for Rock Sample

Figure 14. Control Room

Feed force is determined by the hydraulic pressures, hold down and hold back, in a feed cylinder in combination with a constant test stand weight. Hold down pressure is the hydraulic pressure on the top side of the feed cylinder while hold back pressure is the hydraulic pressure on the bottom side of the feed cylinder. In combination, these two measurements determine the feed force. The hydraulic pressures are set and maintained with valves controlled by automated regulators. These pressures are monitored and recorded during each test run to ensure consistency.

Each performance test is started by setting a rotation speed along with holddown and holdback pressures appropriate for the desired feed force. Once these values are set, a desired supply pressure is dictated to the automated regulator and initiated. As air flow begins, the drill is slowly lowered to the rock specimen and the automated feed control is allowed to take over. The air pressure is monitored for stabilization. Once the system is stable, data collection is initiated and carried out for the desired test time (10 seconds in this case). Collected data includes: air flow, hammer frequency, and hammer advancement along with the controlled variables previously described.

Each hammer was run three times at five pressure steps from 200 psi to 400 psi (1379 to 2758 kPa) in 50 psi (345 kPa) intervals. At each pressure step, data was recorded for 10 seconds. After each of the three runs on the high temperature hammer, it was disassembled to monitor wear and other types of damage on the internal components. The control hammer was not disassembled because pervious laboratory testing had shown that wear and mechanical damage was not likely. The low temperature prototype hammer was lubricated with ISO 220 Rock Drill Oil injected into the air stream at a rate of 12 cc per minute. The high temperature prototype was not lubricated during the test runs. It should be noted that small amounts of oil may have been in the air system from oil clinging to the drill pipe and bypassed compressor oil.

Results are plotted below:

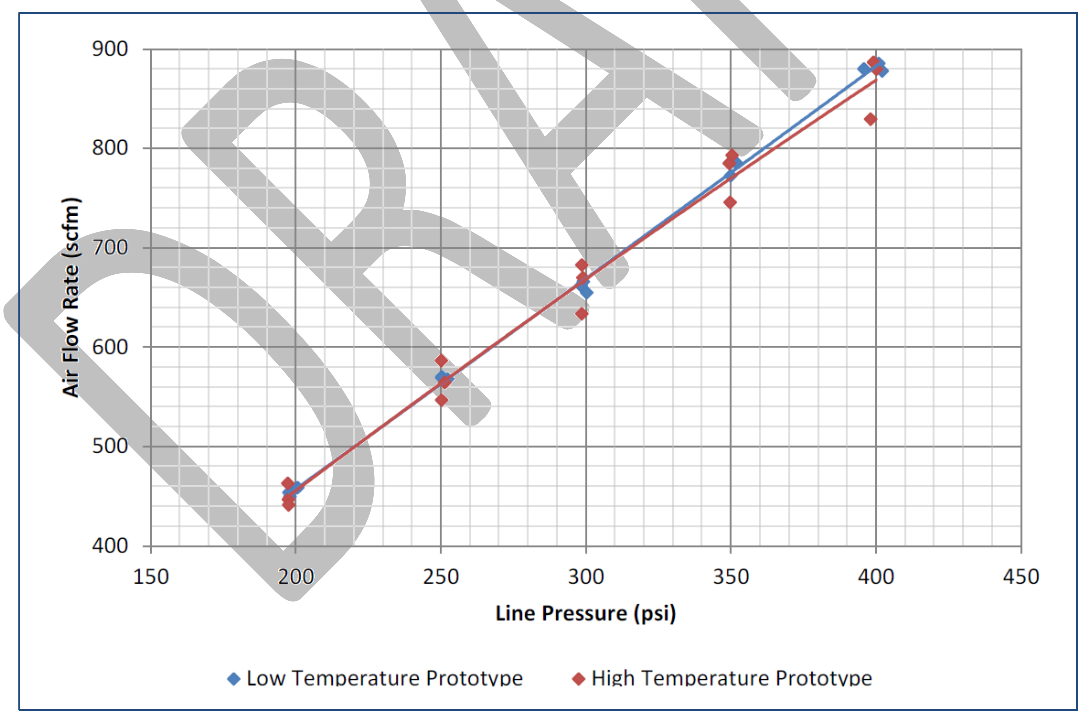

Figure 15. Flow rate vs. backhead pressure comparison for LT and HT prototype

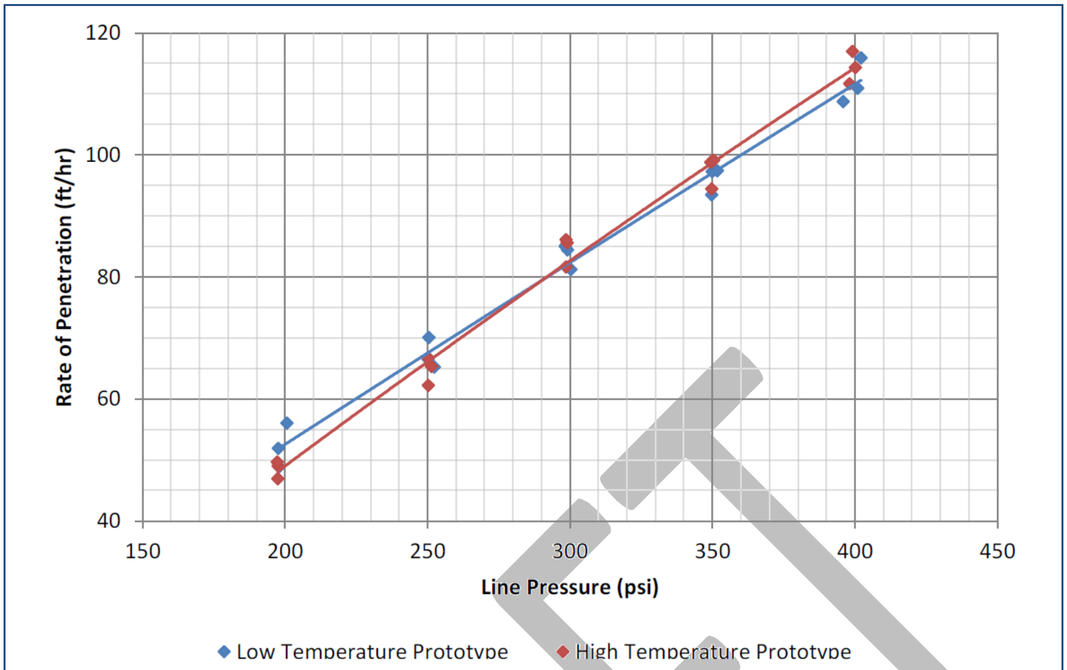

Figure 16. Rate of penetration vs. backhead pressure comparison for LT and HT prototype

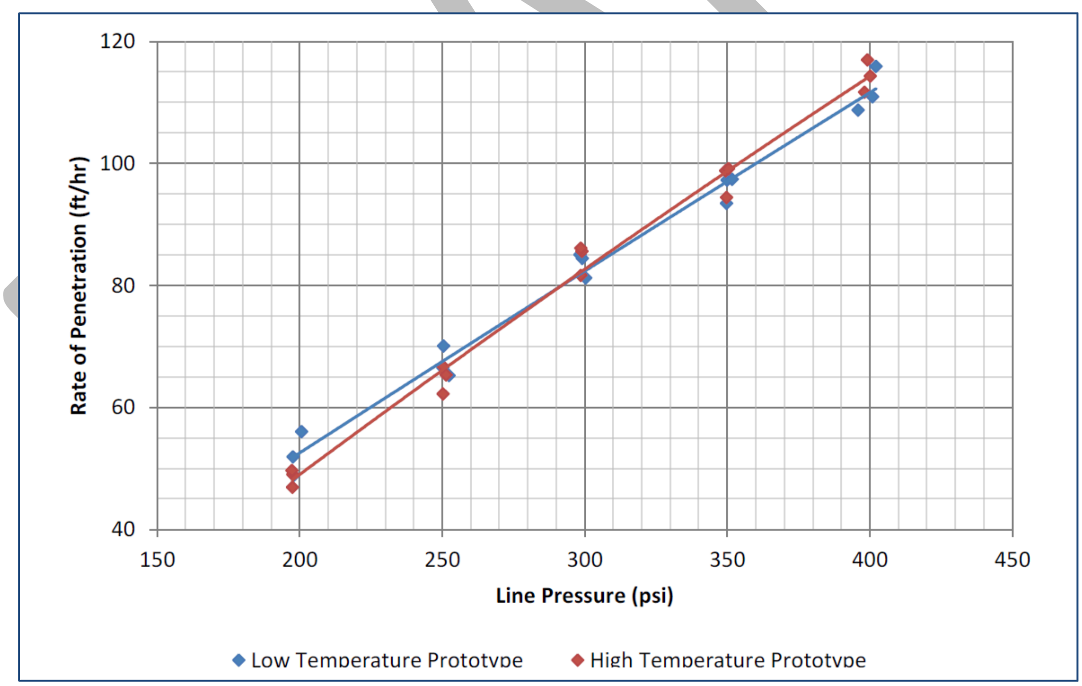

Figure 17. Frequency vs. backhead pressure comparison for LT and HT prototype

The initial performance of the high temperature prototype compared very favorably with that of the low temperature prototype. The slight differences observed are well within normal test variation.

This testing at the Atlas Copco Secoroc test facility validated the performance of the high temperature prototype to be consistent with that of the low temperature prototype, and that no catastrophic failure of parts or the lubricious and wear resistant coating was observed. The high temperature prototype was sent to SNL for both low and high temperature testing at the HOT facility.

3.2 High-Temperature Testing at Sandia

Performance tests were conducted at the high-operating temperature (HOT) facility to validate the data acquisition system and to establish a baseline for hammer performance at various temperatures.

The HOT facility (is a laboratory-scale drill rig that allows borehole thermal conditions to be simulated while drilling. It consists of a drill structure, an integrated data acquisition and control system, a 9kW heating chamber, and a 190kW process gas heater.

Figure 18. Interior of HOT facility

The hammer heater/diverter is designed to serve multiple purposes in the HOT facility. First and foremost, it heats the hammer to simulate downhole temperatures in a geothermal environment. The hammer consists of six 1.5 kW band heaters surrounding a metal shell. The 9 kW heater is designed to heat the hammer to 572°F within one hour. The heater can be controlled directly on the front panel or remotely via TCP/IP.

The secondary functions of the heater/diverter are to control cuttings and prevent the rock from bouncing during drilling. Internally, the diverter has two packing gland seals designed to prevent dust from escaping during drilling. These packing glands force the cuttings through the exhaust port on the diverter. The diverter is able to generate 3000 lbf of hold-down during drilling. This force helps to create the seal between the rock and the diverter.

The process gas heater is used to simulate the temperature rise of the compressed air driving the hammer as it flows through the drill string in a geothermal environment. It is 190 kW circulation heater capable of heating the process gas up to 572°F. The heater is ASME code-stamped for 600 psi at 900°F. It can be controlled directly from the front panel or remotely via TCP/IP.

Typical drilling rigs or test cells are operated and actuated with hydraulic equipment. Pressurized oil in hydraulic systems present a fire hazard, especially in the vicinity of a heat source. Following a conventional design for those systems would result in a combination of hydraulics and heat sources that would have potentially serious hazards to both property and operators. In order to mitigate these thermal hazards, the HOT facility was designed and built to operate entirely on pneumatics.

Tests were conducted on Sierra White granite blocks sourced from Coldspring quarry in Raymond, California. The published unconfined compressive strength of the rock is 23.8 ksi.[1] Verification tests were run at a target pressure of 300 psi to determine flow, frequency, and rate of penetration (ROP). The rotation rate was set to 40 rpm with the WOB at 4000 lbf. The hammer temperature was set to 400°F with process air temperature values of 200°F, 300°F, and 500°F. Approximately 10 seconds of data was collected for each run. The temperature of the hammer was measured with a thermocouple located within the heating chamber. The results from the characterization tests are shown below. The low-temperature prototype was used in the early tests. The process gas was supplied from a portable fixed pressure, high-flow air compressor.

[1] http://www.coldspringusa.com/Building-Materials/Products-Colors-and-Finishes/Granite/Sierra-White/

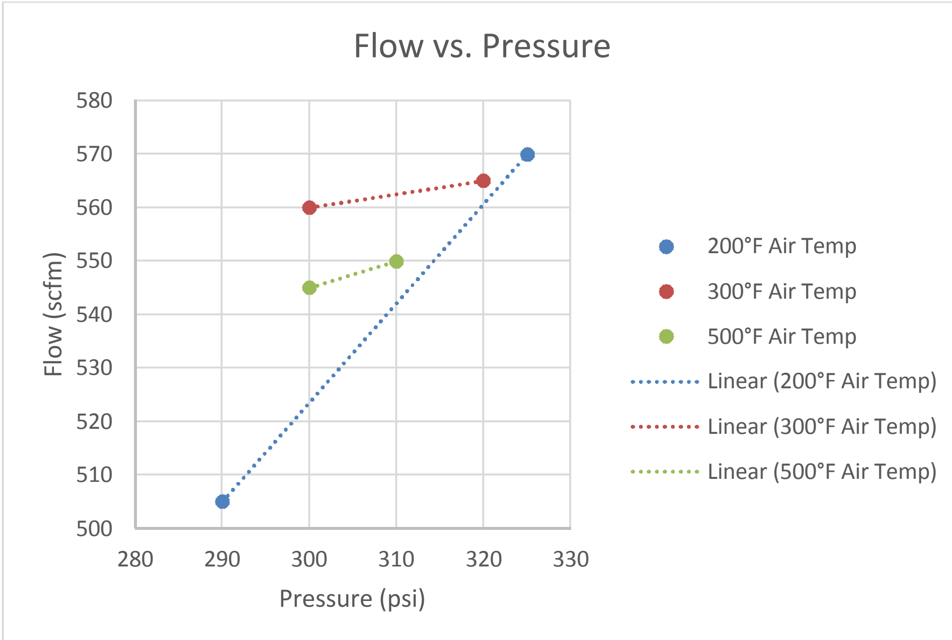

Figure 19. Flow vs. pressure test results for HOT facility characterization

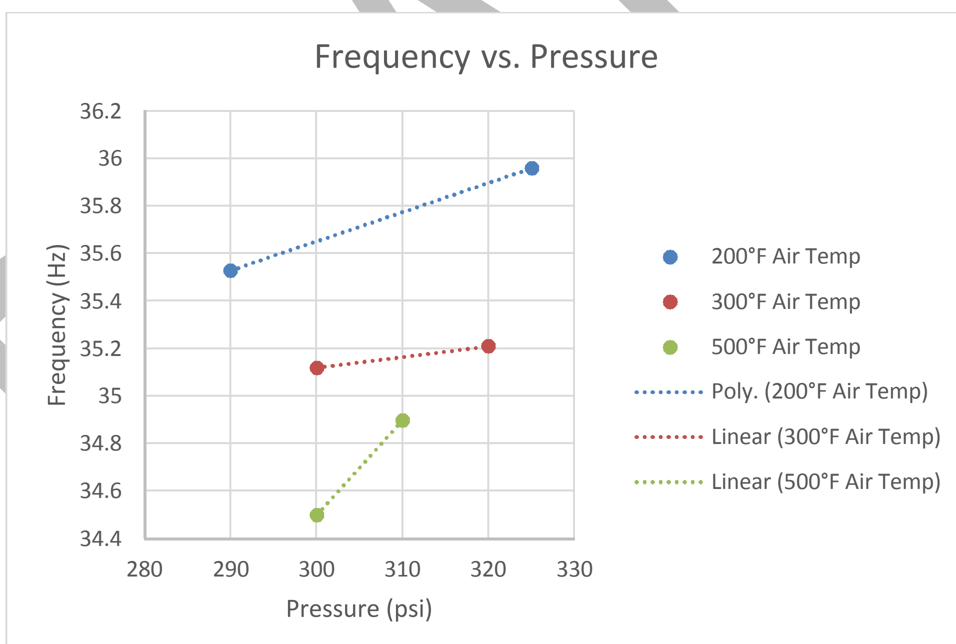

Figure 20. Frequency vs. pressure test results for HOT facility characterization

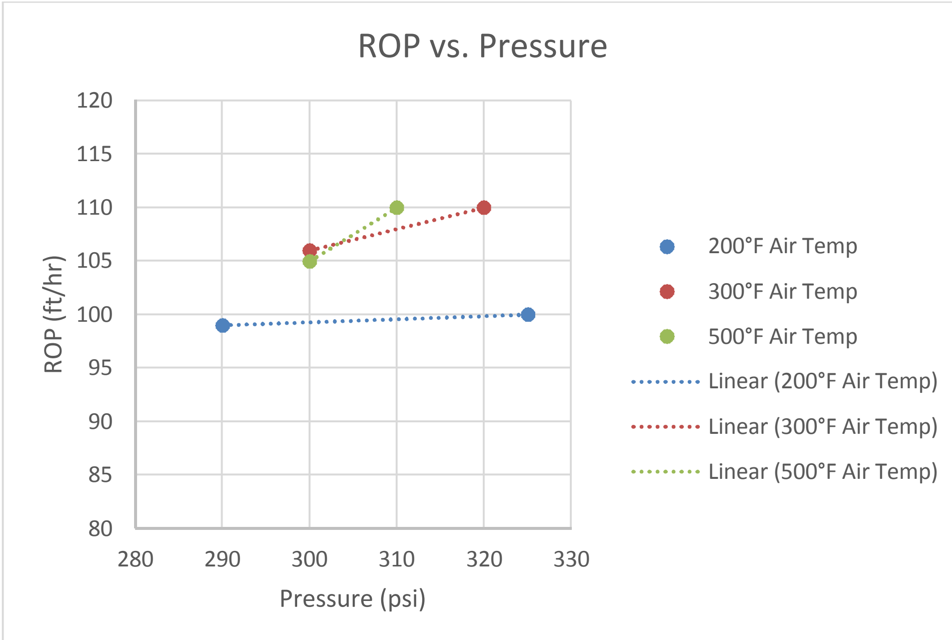

Figure 21. ROP vs. pressure test results for HOT facility characterization

These tests captured in the previous figures were conducted early in the development of the HOT facility. At the time the data was collected, pressure, RPM, and WOB were in open-loop control. There is some drift from test to test in the actual pressure values. Overall, the trends and values of performance are consistent with the results collected in the Atlas Copco test cell.

After the initial tests were conducted, the hammer was disassembled and visually inspected. Figure 22-Figure 24 show the effect of elevated temperatures on conventional lubricants and the hammer components. Residual lubricants from the initial assembly become solid and leave a solid film on the hammer air cylinder and piston.

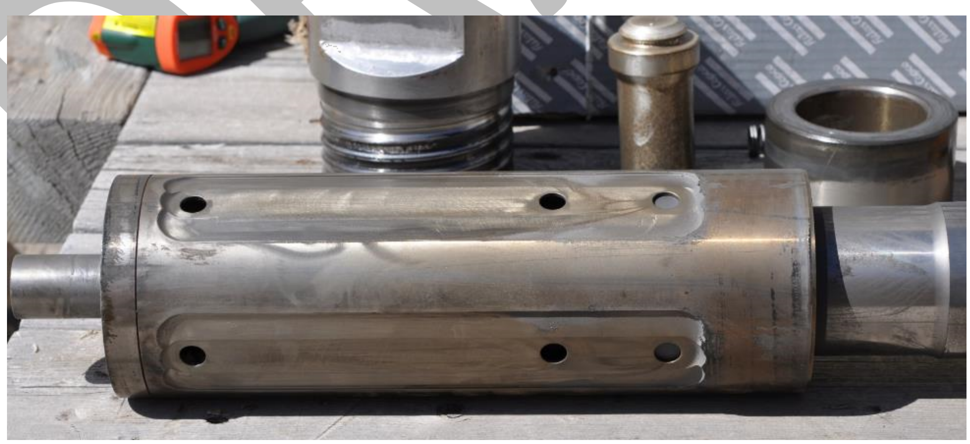

Figure 22. Piston sleeve assembly after operating at 400°F

Figure 23. Piston sleeve inner diameter after operating at 400°F

Figure 24. Piston with no lubrication at 400°F

After verifying the performance of the HOT facility control and DAQ system, tests on the high-temperature prototype were conducted. In addition to characterizing the hammer performance, durability of the piston material and coating were also evaluated.

3.2.1 <u>High-temperature (HT) piston results</u>

The high-temperature tests were conducted across a range of hammer temperatures and air pressures. The rotation rate was set to 40 rpm with the WOB at 4000 lbf. Air pressure pressures ranging from 200 to 350 psi to determine flow, frequency, and rate of penetration (ROP). The hammer temperature was set to between 400°F and 450°F with process air temperature values ranged from 150°F to 550°F.

Initial tests with the HT parts showed that drilling performance was comparable with standard operating conditions. However, there was rapid wear on the struck end of the piston. The progression of wear on the HT piston is illustrated in Figure 25. Through the early tests, the hammer was disassembled frequently to assess the wear rate of the coating. The first inspection was performed after 36” of drilling at 400°F. The inspection revealed dramatic wear of the coating and base material at the stem end of the piston. The other rubbing sections of the piston showed no signs of wear.

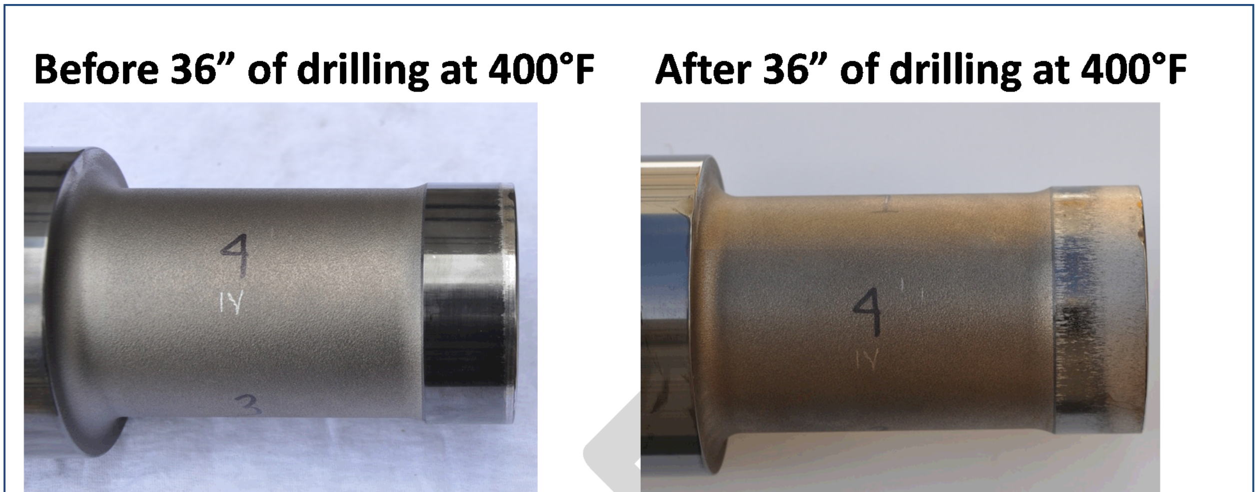

Figure 25. Stem end of HT piston with solid lubricant

Subsequent inspections were conducted at longer intervals after the initial inspection to allow more footage to be drilled. The coating on the stem was completely worn away after 27 feet. Additional wear patterns began to develop on the mid-section of the piston.

The high-temperature piston showed signs of galling and excessive wear early on. The lower hardness of the material (~HRC 46) compared to the conventional material selection was the cause of the high levels of wear. Test of the high-temperature piston was abandoned in favor of coating the low-temperature piston with the same lubricious coating.

3.2.2 Standard (LT) piston with coating results

Previous coupon-level material tests indicated that a hardened surface would provide a solid substrate for the DLC and barrier layer. Although the tempering temperature of the standard piston material was a possible concern, the known hardness of the low-temperature material made it a good candidate for testing the coating at temperature.

In addition to addressing the material hardness, several geometric changes were made to the piston to reduce contact stresses along sliding surfaces. A chamfer was added to the leading edge of the piston. A radius was added to the leading edge of the mid-section of the piston where it enters the air cylinder. The same hammer components were used from the previous tests. A picture of the coated LT piston is shown in Figure 26.

Figure 26. LT piston with DLC coating applied

At least three runs were made at were made at pressure set points to evaluate the performance. Hammer temperature ranged from 400°F to 572°F. Air pressure was varied from 200 psi to 300 psi. Process gas temperatures varied from 150°F to 500°F. Additional runs were made to reach total footage of approximately 200 ft.

Hammer performance results are captured in Figure 27-Figure 29. The plots include data from all the runs at the various soak and process gas temperatures. The overall performance of the hammer at temperature is consistent with the measured performance at the Atlas Copco test cell.

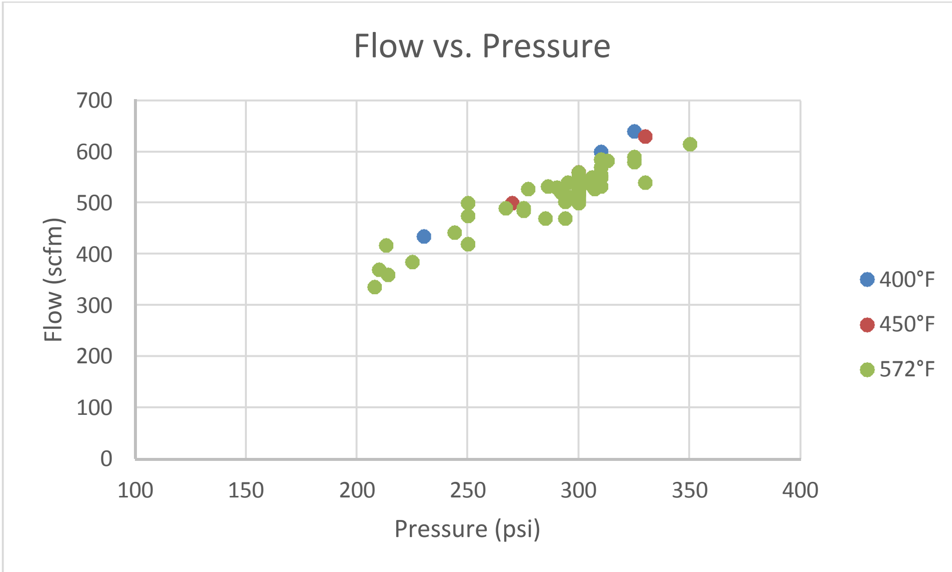

Figure 27. Flow vs. pressure for all LT piston tests

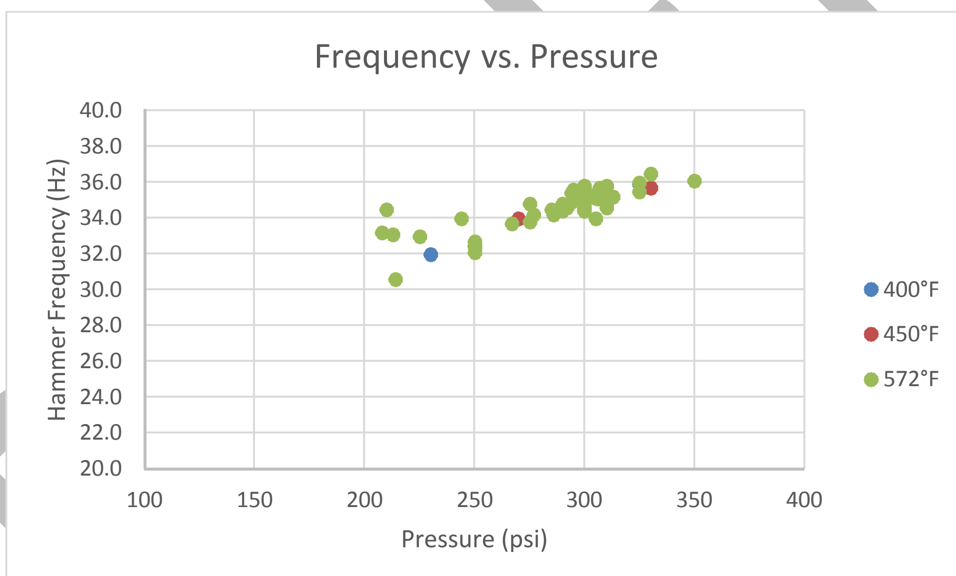

Figure 28. Hammer frequency vs. pressure for all LT piston tests

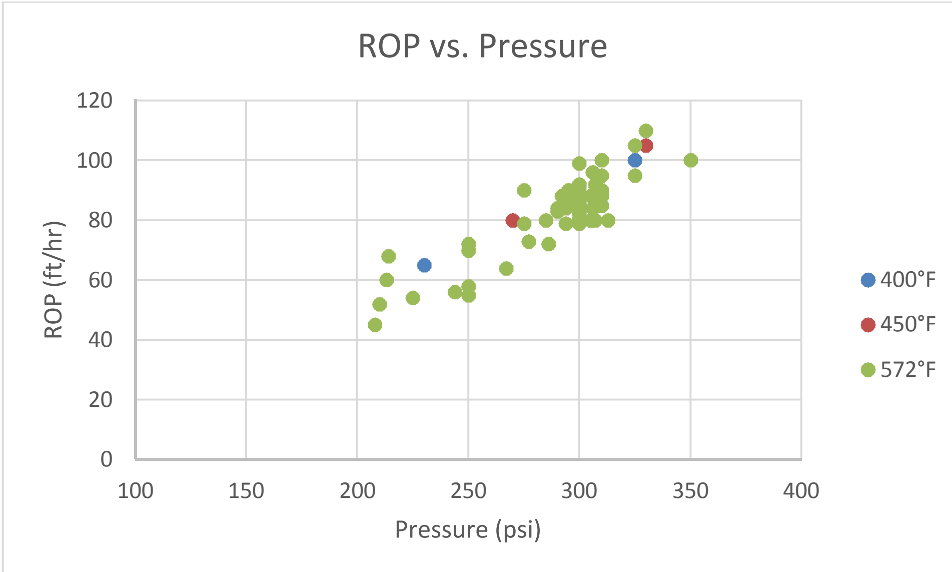

Figure 29. ROP vs. pressure for all LT piston tests

Similar to the tests with the high-temperature piston, the low-temperature piston hammer was disassembled and inspected at specified intervals. The intervals at the start of the tests were shorter due to uncertainty in how the piston would behave. The results from first test interval are shown in Figure 30.

No visible signs of wear were apparent after the initial test interval. This early performance allowed inspection intervals to be extended. Those intervals varied throughout testing due to timing and coordination of the rock samples being drilled.

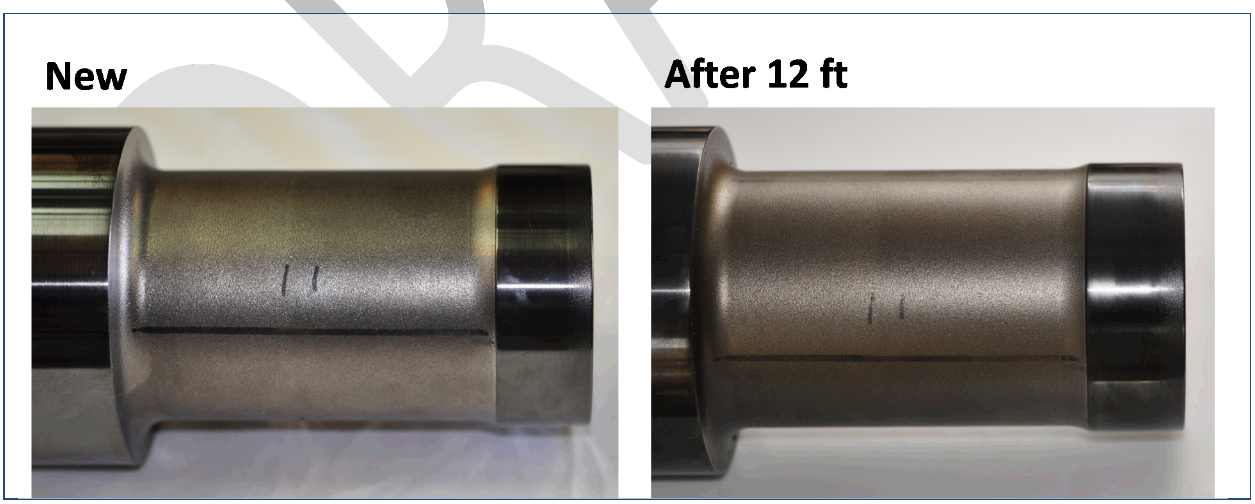

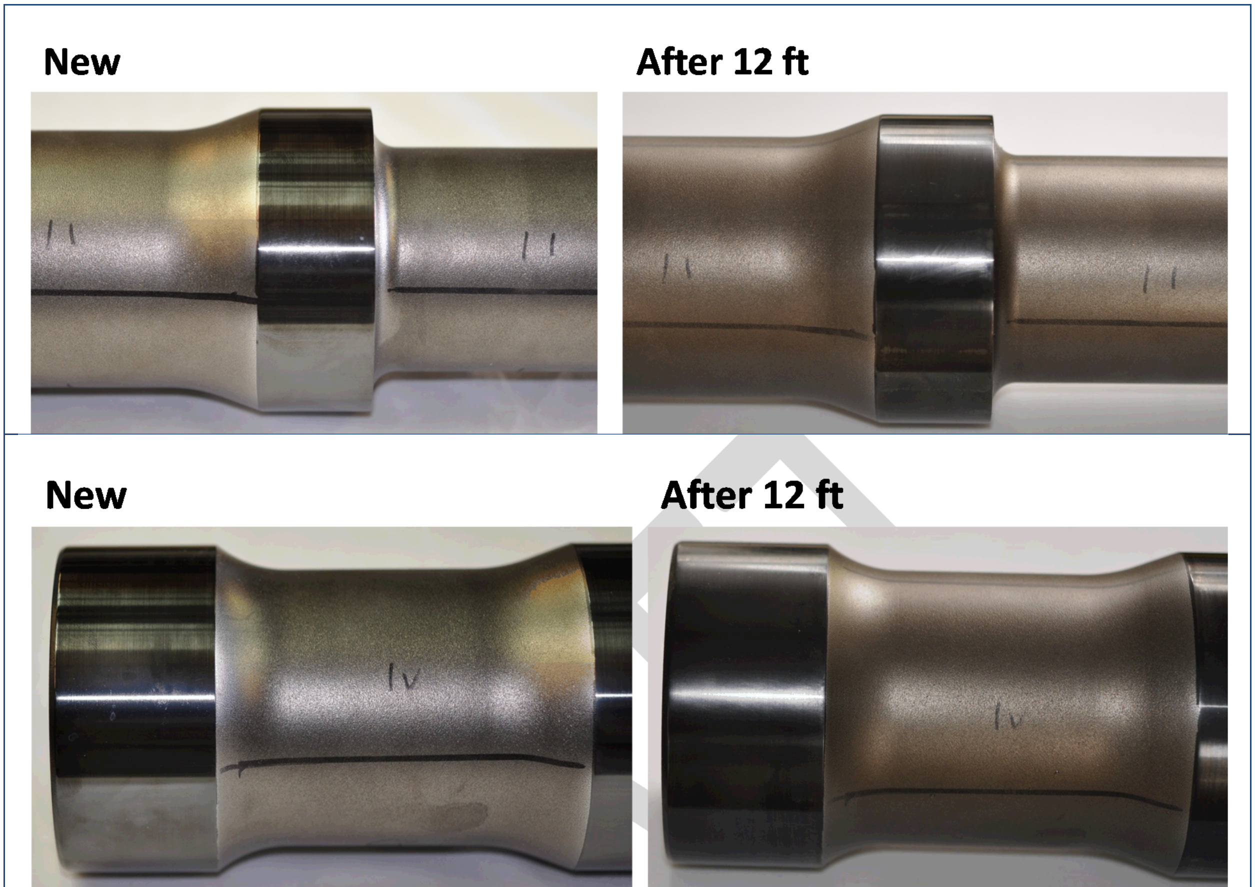

Figure 30. LT piston with DLC coating applied

The wear patterns that developed in the previous intervals are more prominent after the 119 ft interval inspection. The tempered region has expanded towards the struck end of the piston. On the struck end, bare metal is visible in Figure 31. The wear pattern is non-uniform around the circumference.

The wear patterns were inspected under a microscope to provide a better understanding of the phenomenon. On the fare end of the piston, the wear marks are perpendicular to the axis of the piston. This indicates that the wear is due to the piston sliding within the air cylinder. This is to be expected since this is the normal motion of the piston.

In the mid-section and struck end, source of the wear is not as clear. The magnified images show the original machining marks being burnished away. This process could be the result of a combination of the piston rotating and sliding within the hammer case.

After 119 ft

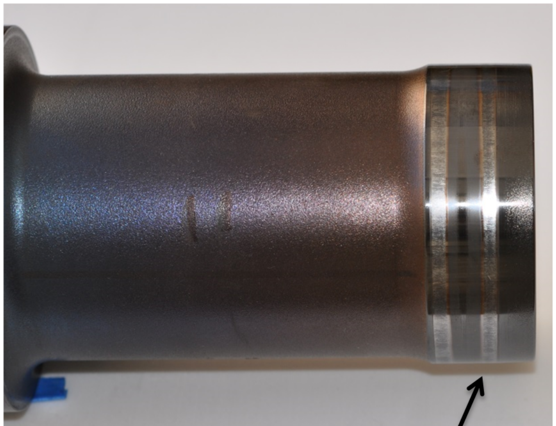

Additional wear

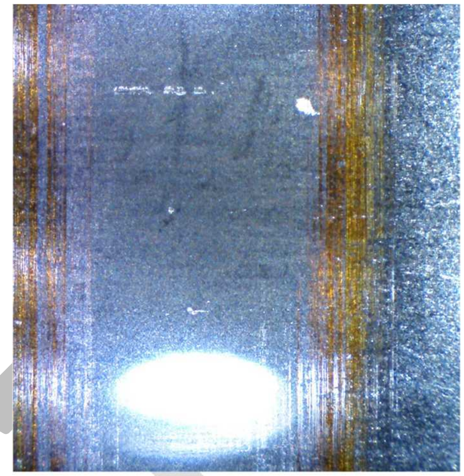

50x zoom of stem end

After 119 ft

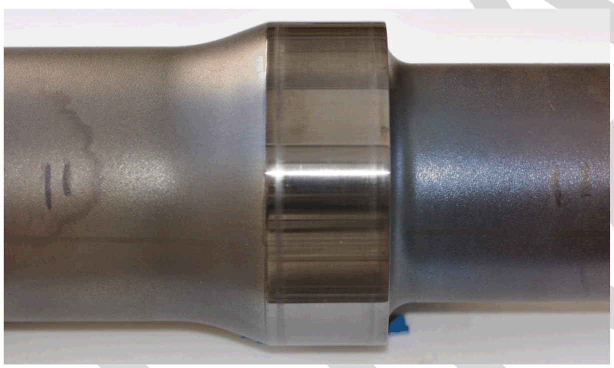

- Wear locations consistent with 40-58

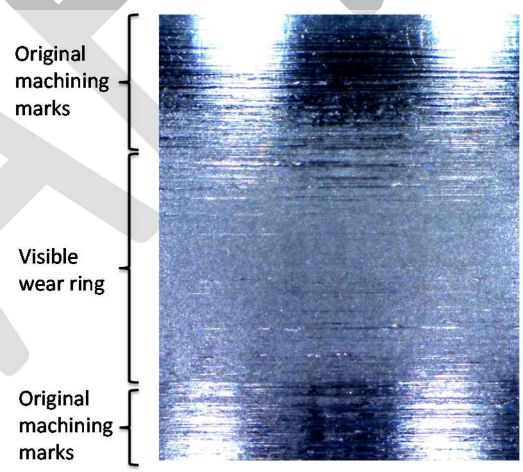

50x zoom of wear ring on mid-section of piston

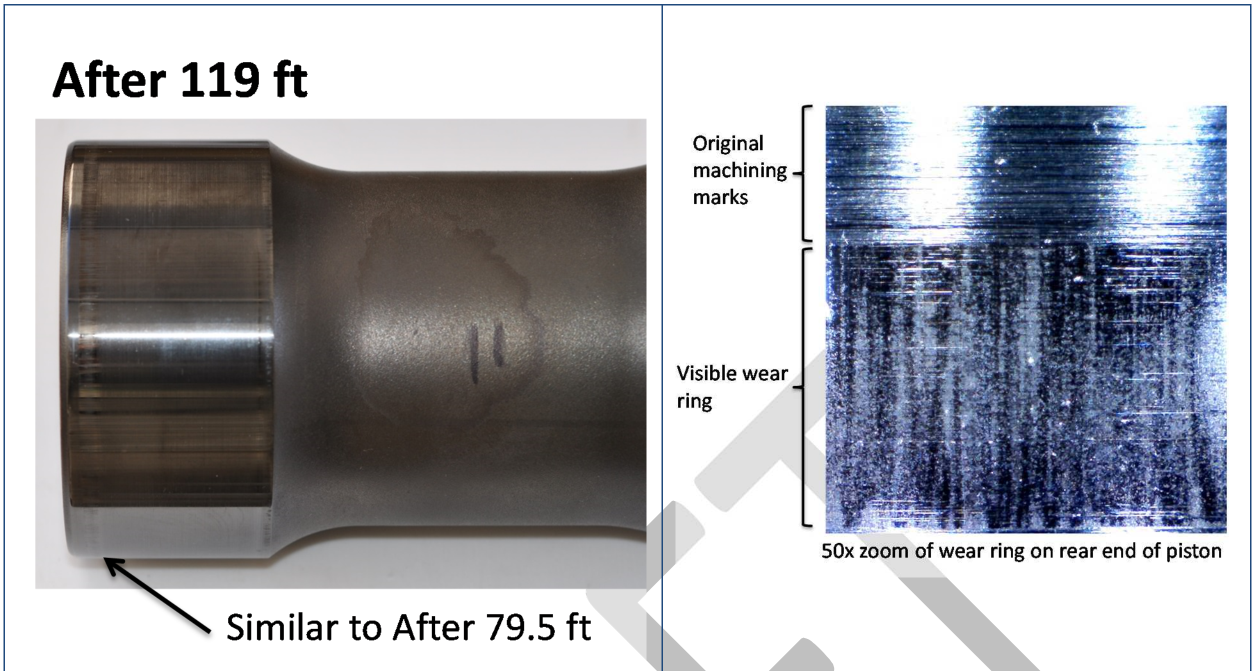

Figure 31. LT piston with DLC after 119 ft.

The check valve is shown in Figure 32 to illustrate the elevated temperatures seen within the hammer. The check valve is located within the hammer and sees direct heat from the process gas air. The deep blue color indicates sustained temperatures in the range of approximately 550°F-600°F.

Figure 32. Check valve tempering temperature color change

The next inspection shows a steady progression of wear that was seen in the previous interval. The tempered region continued to expand towards the struck end. The wear bands on the stem appear more polished. The transverse wear pattern visible on the far end in the previous interval is now visible in the mid-section.

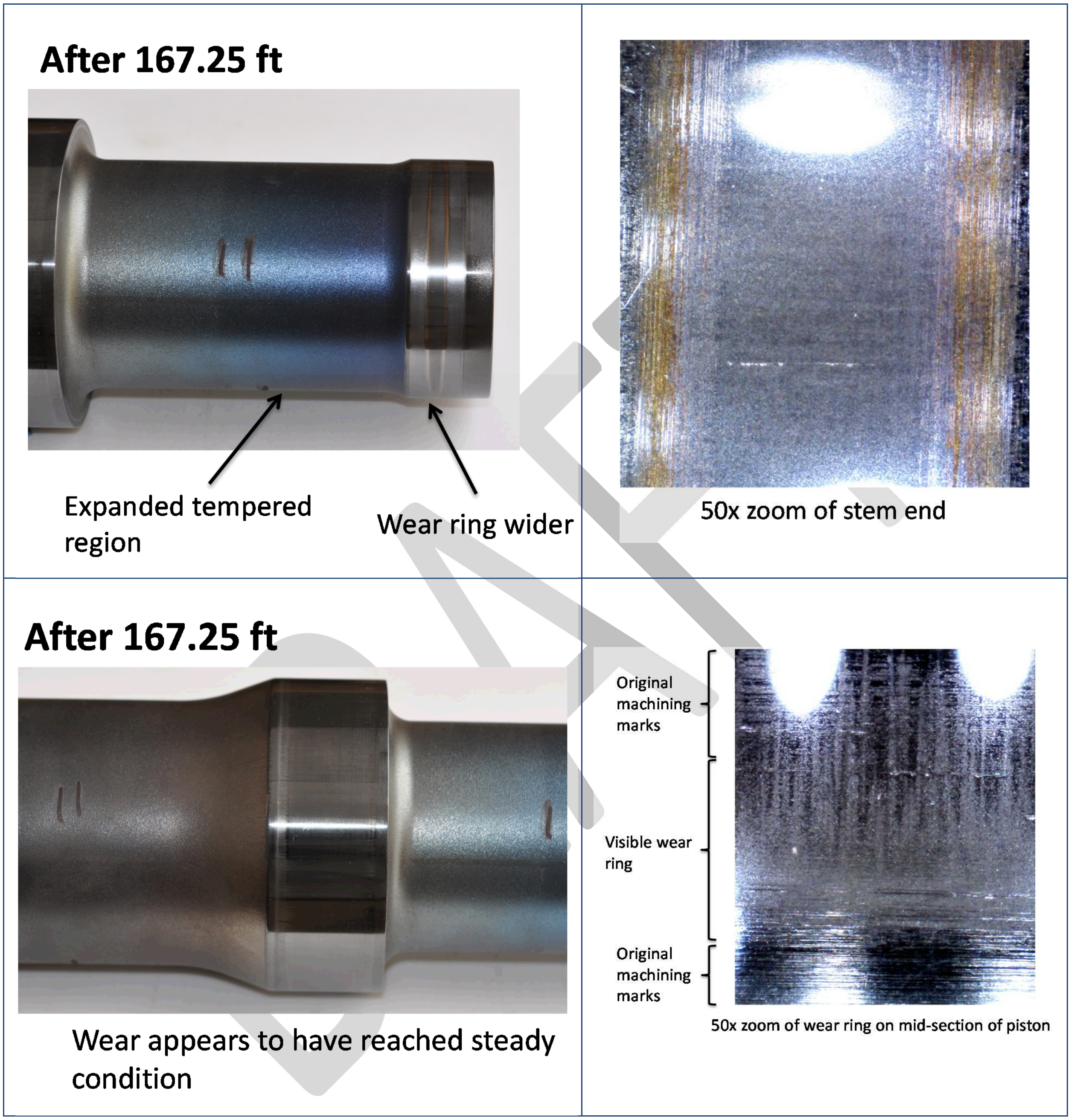

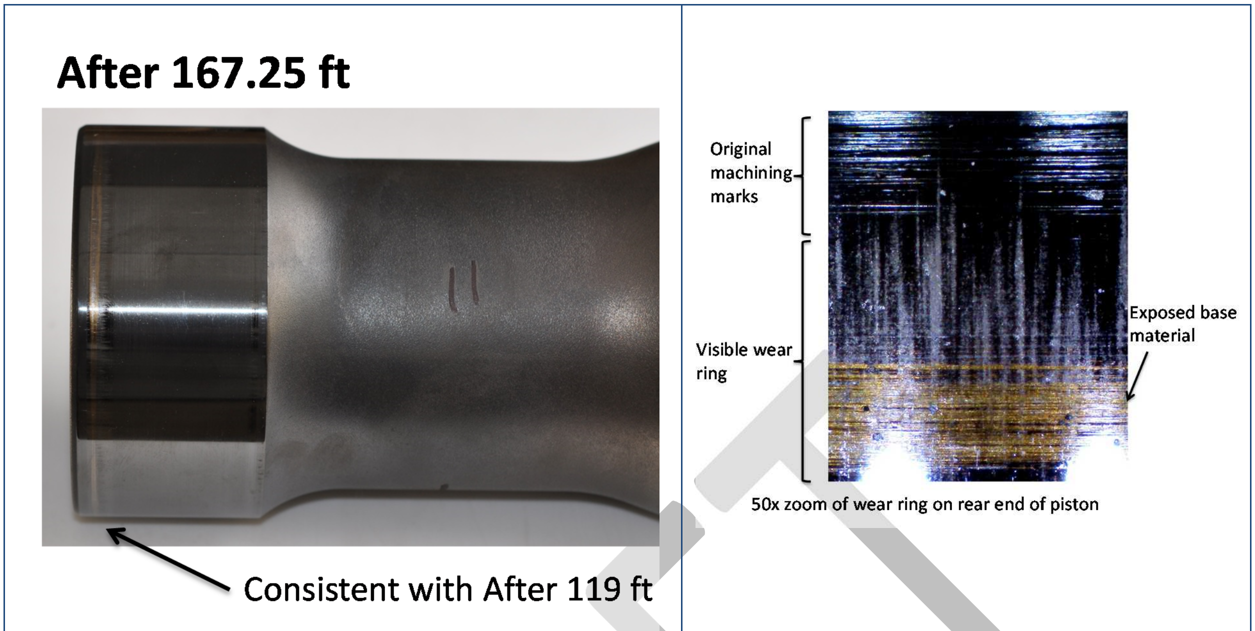

Figure 33. LT piston with DLC after 167.25 ft.

The final inspection revealed additional wear on the stem end. The two wear rings have nearly coalesced. A band of the original coating remains in place. The transverse wear patterns in the mid-section and the far end have expanded. There is a visible ring on the far end of the piston indicating material transfer between the air cylinder and piston.

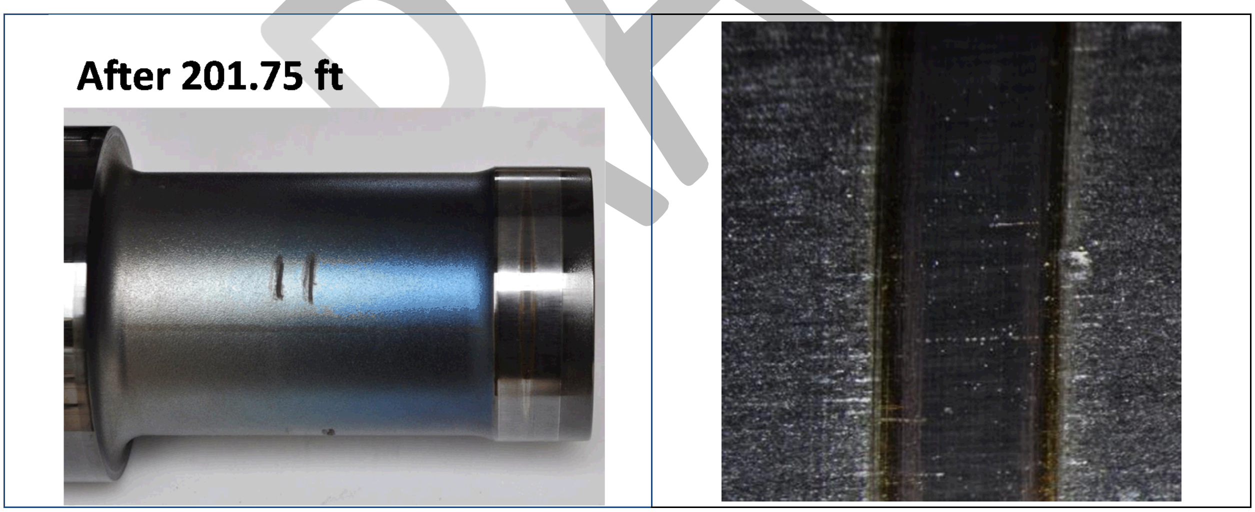

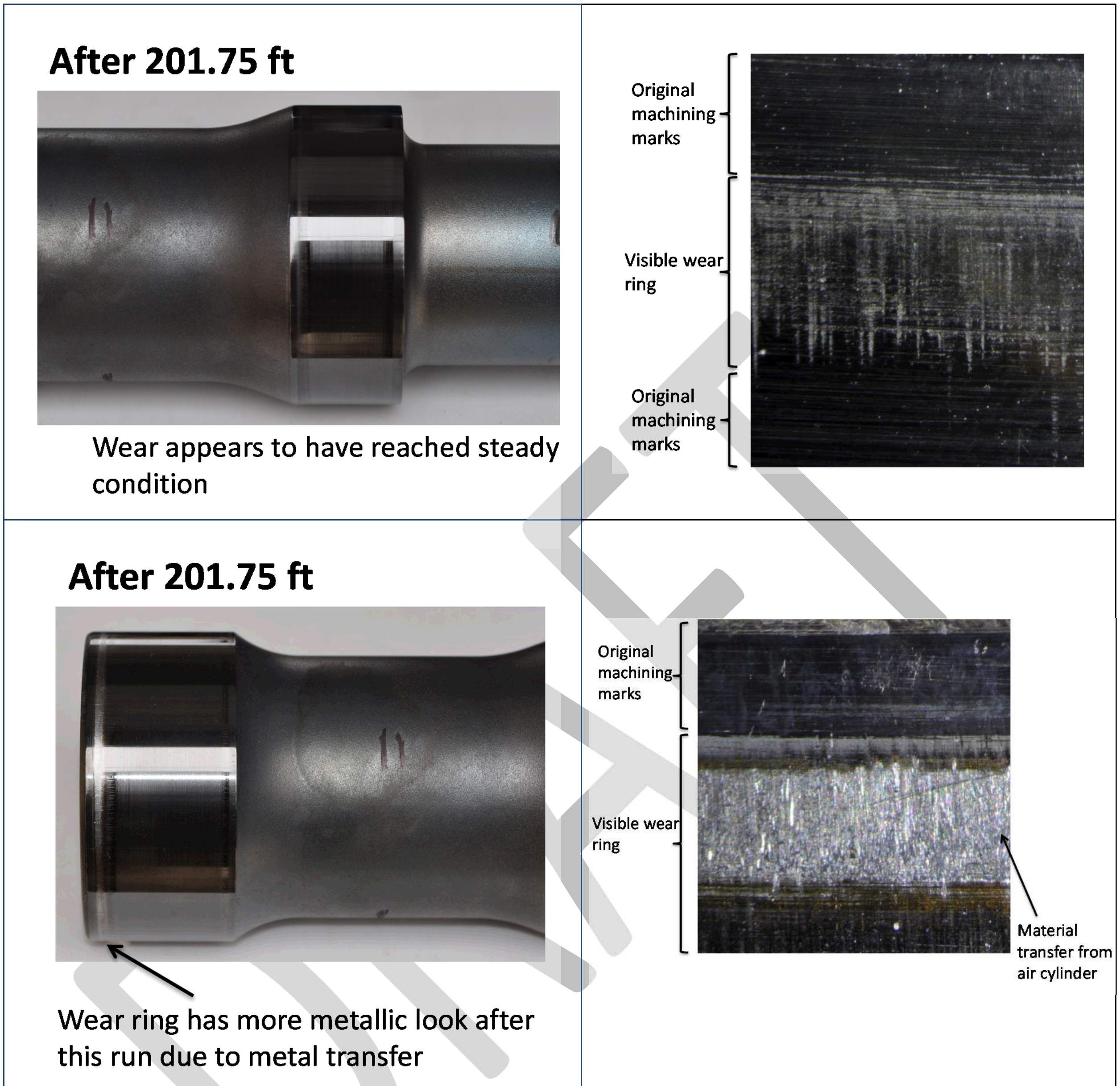

Figure 34. LT piston with DLC after 201.75 ft.

Overall, the hammer configuration with the LT material piston and HT material distributor drilled more than 200 ft. in 24 ksi Sierra White granite at temperatures up to 572°F without liquid lubricants. During this time, it went through multiple thermal cycles and was able to maintain performance with rates of penetration exceeding 100 ft/hr. Although wear patterns developed on the moving parts, the performance of the hammer was quite remarkable when considering the operating environment.

4. Discussion

The initial efforts in the Advanced Percussive Drilling Technology were focused on demonstrating the feasibility of a high-temperature hammer. Early testing showed that developing a hammer without elastomers used in the timing scheme was possible.

Computational modeling of the hammer performance was used to define the timing ports for the hammer. Leak paths and other issues were identified and resolved, and the prototype was tested in the Atlas-Copco test cell. Performance levels were comparable to conventional hammers. Elevated temperature testing highlighted the importance of lubrication on the internal components.

The initial material selection for the high-temperature piston lacked sufficient surface hardness. Although the hammer performance was in line with the low-temperature prototype, the excessive wear on the piston sliding surfaces was deemed unacceptable. The testing with the high-temperature piston, was not however a total loss. The wear patterns that developed on the softer piston material proved to be beneficial in identifying areas and geometries that were experiencing high contact forces.

Based on those test results, modifications to the piston geometry were made to improve the wear characteristics of the sliding parts. Modifications to the piston geometry and material selection proved to be effective. The coating wear rate on the struck end of the piston was higher than the other sliding surfaces. The wear on the mid-section and far end of the piston reached a steady wear pattern. The multi-layer solid lubricant architecture was effective under the extreme conditions encountered during testing. The performance of the hammer over the approximately 200 feet of drilling remained consistent. Additional field testing will be required to further prove out the tool.

In the end, only one coating and two substrate combinations were tested. Testing additional material and coating combinations could have helped to determine if there are potentially better configurations for operating at high-temperature.

The effect of the process gas temperature on the hammer performance was not immediately clear. The relationship between increasing air pressure and higher ROP is the primary effect on hammer performance. The soak temperatures, however appeared to cause changes to the underlying component material. The "bluing" of the steel was a clear indication that the piston and other hammer components were reaching a tempering temperature.

Although the primary focus of the project was developing a percussive hammer capable of operating at high-temperatures seen in a geothermal environment, a significant portion of the project was dedicated to developing the elevated temperature test capability. The development of the HOT test facility was an exercise in both design and system integration. The extreme conditions required specialized solutions for drill actuation, plumbing, and operator safety. Successful deployment and integration of multiple sub-systems was required to meet the project objectives of testing at 300°C (572°F).

5. Conclusions

The high-temperature DTH development effort encompassed both tool development and manufacturing as well as building a unique test capability. Material and lubrication issues were addressed and evaluated. Alternative hammer designs were tested and validated. The effect of temperature on DTH performance was captured in lab-based testing. The results show that a high-temperature DTH is a viable tool for the right conditions. However additional testing needs to be conducted to determine the durability and reliability of the tool prior to full-scale deployment. The authors are looking forward to future opportunities to field the tool and advance the technology readiness levels for commercial use.

6. Acknowledgements

The authors would like to acknowledge the help of co-workers at Sandia and Atlas-Copco in support of the work. They include Michael White, Paul Campbell, Ron Boyd, Kelly Ferguson, and Trevor Jones from Atlas-Copco and Doug Blankenship, Jeff Greving, Elton Wright, Dennis King, Anirban Mazumdar, Dennis King, Anirban Mazumdar, Steve Buerger, Rand Garfield, Lisa Deibler, and Carlos Medrano from Sandia.

REFERENCES

Kahraman, S., N. Bilgin and C. Feridunoglu (2003). "Dominant rock properties affecting the penetration rate of percussive drills." International Journal of Rock Mechanics and Mining Sciences **40**(5): 711-723.

Polsky, Y., Louis Capuanao Jr., John Finger, Michael Huh, Steve Knudson, A.J. Chip Mansure, David Raymond, Robert Swanson (2008). "Enhanced Geothermal Systems (EGS) Well Construction Technology Evaluation Report." SANDIA REPORT(SAND2008-7866).

Thuro, K. (1996). "Drillability Prediction - Geological Influences in Hard Rock Drill and Blast Tunneling." International Journal of Earth Sciences **86**(2): 426-438.